Journal of Physics: Conference Series **250** (2010) 012028 doi:10.1088/1742-6596/250/1/012028

Effective Management of FXG Gel Dosimetry

T Olding[1], J Darko[2] and L J Schreiner[1,2]

[1]Department of Physics, Queen's University, Kingston, Ontario, Canada, K7L3N6
[2]Cancer Centre of South Eastern Ontario at Kingston General Hospital, 25 King Street West, Kingston, ON, Canada, K7L5P9

E-Mail: Tim.Olding@krcc.on.ca

Abstract. The details of a calibration basis for the Fricke-xylenol orange-gelatin (FXG) gel dosimeter combined with the fast, easily accessible readout tool of cone beam optical computed tomography (CT) are described in this report. With proper controls in place, the results from a test intensity modulated radiation therapy (IMRT) treatment plan evaluation indicate that greater than 95% Low's gamma function agreement between plan and gel-measured dose using 3% dose and 3 mm distance-to-agreement criteria is achievable.

1. Introduction

This paper discusses some of the important parameters for ensuring the reliability of cone beam optical CT-based FXG gel dosimetry. Results are presented that establish the intra-batch reproducibility, dose calibration linearity, and megavoltage range energy independence of the dosimeter using a Vista^{TM} cone beam scanner (Modus Medical Devices Inc, London, ON, Canada) for optical readout [1]. Time and temperature control criteria are set to manage the dosimetry. A dosimeter modification is then described that reduces stray light perturbation in the optical readout of a standard-sized FXG gel-filled 1 L polyethylene terephthalate (PETE) jar dosimeter and improves the overall three dimensional (3D) dose measurement.

2. Experiment

2.1. Dosimeter Preparation & Imaging

FXG gel dosimeters were prepared according to the recipe outlined by Babic *et al* (2008). After preparation, the heated formulations were poured into standard-sized 1 L PETE jars and allowed to set overnight in a refrigerator prior to irradiation. Dosimeter imaging was performed using the Vista scanner set to a camera lens aperture of f5 and 590 nm LED illumination. Reference scans were completed on the dosimeters prior to irradiation at the highest shutter exposure time possible without inducing camera pixel saturation (and the lowest gain setting) in approximately 4 minutes. After irradiation, data scans were acquired at the same camera settings as the reference scans. Optical CT attenuation images were reconstructed to an isotropic voxel resolution of 0.5 mm, unless otherwise specified. The remaining details of scanner operation are specified elsewhere [1]. Temperature measurements were taken using a digital temperature probe (TM99A-NA Digital Thermometer, Nuclear Associates, Carle Place, NY, USA). Line profiles and regions of interest in the reconstructed optical CT images of the FXG gel dosimeters and gelatin phantoms were evaluated using Microview 2.1.2 (GE Healthcare, United Kingdom) or MatLab (Mathworks, Newark, NJ, USA) software.

2.2. FXG Gel Calibration

Gel irradiations were completed on the day after manufacture using a Varian Clinac 21iX linear accelerator (Varian Medical Systems, Palo Alto, CA, USA), or a Gulmay superficial x-ray therapy system (Gulmay Medical Inc, Buford, GA, USA). Depth fiducials were marked on the FXG-gel filled 1 L PETE jars in permanent marker, serving as reference points for registration of depth dose to attenuation in the reconstructed optical CT image. Calibration 6 x 6 cm photon and electron beams were delivered to the top surface of the gel-filled PETE jar with the lid off (typically to a maximum absorbed dose of 180-210 cGy) using the Clinac irradiator. A 200 cGy, 80 kVp delivery was performed using the Gulmay unit, employing a 6 cm cone set to the gel surface.

Calibration photon beam central axis depth dose data were obtained from 0.13 cm^3 ionization chamber-water tank measurements (CC13/TNC ionization chamber, Scanditronix-Wellhofer North America, Bartlett, TN, USA). Calibration electron beam central axis depth dose data were acquired from diode-water tank measurements (DEB002-3727, DEB022-3608, Scanditronix-Wellhofer North America). The dose data were considered to be accurate to within an uncertainty of ± 0.5% based on standard deviation of the measurement. The irradiator room temperature was not specified, but the gel dosimeters were kept in a covered holding tank filled with water maintained to 20.0-21.0 ± 0.2°C until the point of irradiation.

Figure 1a shows raw FXG gel calibration data for a range of beam energies, corrected for auto-oxidation during the time between the reference and data scans [2]. Optical CT scans of the gels were acquired at 30 ± 0.2 minutes post-irradiation in the temperature range of 20.8-21.2 ± 0.1°C. Each attenuation data point was obtained as the mean value of a 5 mm diameter single slice circular region-of-interest on the central depth dose axis of the electron (or photon) beam in the optical CT volume image. Electron beam calibrations for two dosimeters prepared from the same gel batch and irradiated with a 200 cGy, 6 x 6 cm, 20 MeV electron beam at two different dose rates are also shown in figure 1a (inset). At each depth, the mean optical attenuation values from these two dosimeters were observed to be linear and in agreement within error over the full dose-to-attenuation calibration range. Figure 1b shows the agreement between Wellhofer ion chamber-measured and linear dose-to-attenuation fit-calibrated FXG gel depth dose curves.

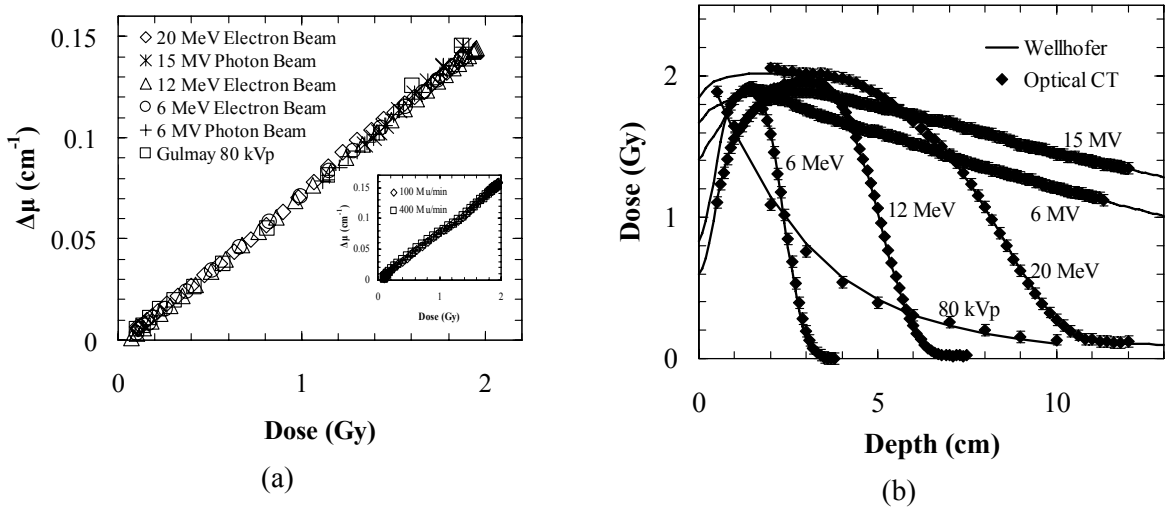

Figure 1: (a) Calibration data corrected for auto-oxidation, showing the reproducibility and energy independence of the FXG gel dosimeter. The inset plot shows the 20MeVelectron beam calibration of two dosimeters from same gel batch, delivered at different dose rates. (b) Depth dose curves of the different treatment beams from (i) the Wellhofer measurements in a water tank, and (ii) the calibrated FXG gel dosimeter (assuming a linear calibration relationship between absorbed dose and optical attenuation). For the purpose of clarity, only the line through the Wellhofer depth dose data is shown in this plot.

2.3. Time and Temperature Controls

To examine time-based changes in the dosimetry, a FXG gel-filled 1 L PETE jar was irradiated to a surface dose of 200 cGy on the day after manufacture using the Gulmay unit with a 6 cm cone insert, then imaged over a period of 24 hours. The dosimeter was kept in a covered water bath held at 20.1 ± 0.2°C between scans and the scanner matching tank fluid was held at 20.1 ± 0.2°C during each scan. The central axis depth attenuation curves adjusted for auto-oxidation of the dosimeter [2] clearly show dose development over this time period, at a rate of approximately 2.8-3.0% per hour (figure 2a). Another time-sensitive factor seen in the dosimeter is the loss of spatial dose integrity over time due to diffusion of the ferric ion-xylenol orange dye complex [3]. For example, at the representative depth of 1 cm, the normalized attenuation changes in magnitude approximately at a rate of 0.5% every 10 minutes at the most rapidly changing point in the profile through the diameter of the jar image.

To quantify the influence of dosimeter temperature at the time of optical scanning, a FXG gel was pre-irradiation imaged at 22.0 ± 0.1°C, irradiated with a 6 x 6 cm, 20 MeV electron beam to a dose of 200 cGy at a reference depth of 3 cm, then post-irradiation imaged at different dosimeter temperatures (1 mm reconstruction cubic voxel size, see figure 2b). Note that the dosimeter was refrigerated for 3 weeks prior to post-irradiation scanning to ensure reaction completion (i.e. dosimeter development was minimal at this point). Individual scans were acquired on the Vista scanner, and auto-oxidation effects were taken into account [2]. Approximate measurements of the dosimeter temperature were acquired prior to each scan by inserting the temperature probe 1 cm into the FXG gel. The temperature of the matching tank solution was held to 22 ± 1°C during the post-irradiation scans.

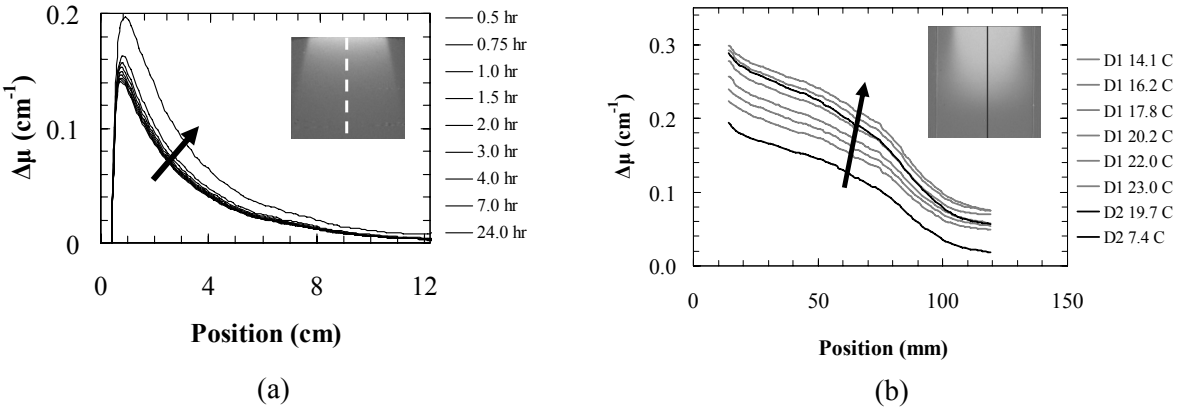

(a) (b)

Figure 2: (a) Attenuation (depth dose) development of an 80 kVp, 200 cGy Gulmay irradiation delivered to an FXG gel dosimeter. The arrow shows increasing time. (b) Central axis attenuation for a FXG gel dosimeter irradiated with a 200 cGy, 20 MeV electron beam. Two sets of scans were obtained for this dosimeter on subsequent days (D1 in gray, D2 in black), with increasing temperature shown by the arrow direction.

2.4. Dosimeter Modification

A number of sources of stray light in the optical measurement system perturb the accuracy of cone beam optical CT-based FXG gel dosimetry. One of the predominant stray light perturbations is angled scatter from the gel-forming matrix. In an effort to better manage this effect, several alternative gel-forming materials were investigated and one (a 300 Bloom bovine bone gelatin from Eastman Gelatine Corp, Peabody, MA, USA) was selected for further evaluation. Figure 3a shows the reconstructed profiles across two 5 wt% gelatin-in-water-filled 1 L PETE jars imaged in the Vista scanner (against a reference scan of the matching tank solution). One of the jars was prepared using the standard 300 bloom porcine skin gelatin and the other from the alternative bovine bone gelatin. Figure 3b shows the molecular weight distributions of these two gelatin materials determined by particle size exclusion chromatography (analysis completed by a third party through Eastman Gelatine Corp). The time at which the signal is observed is correlated against the behavior of the known

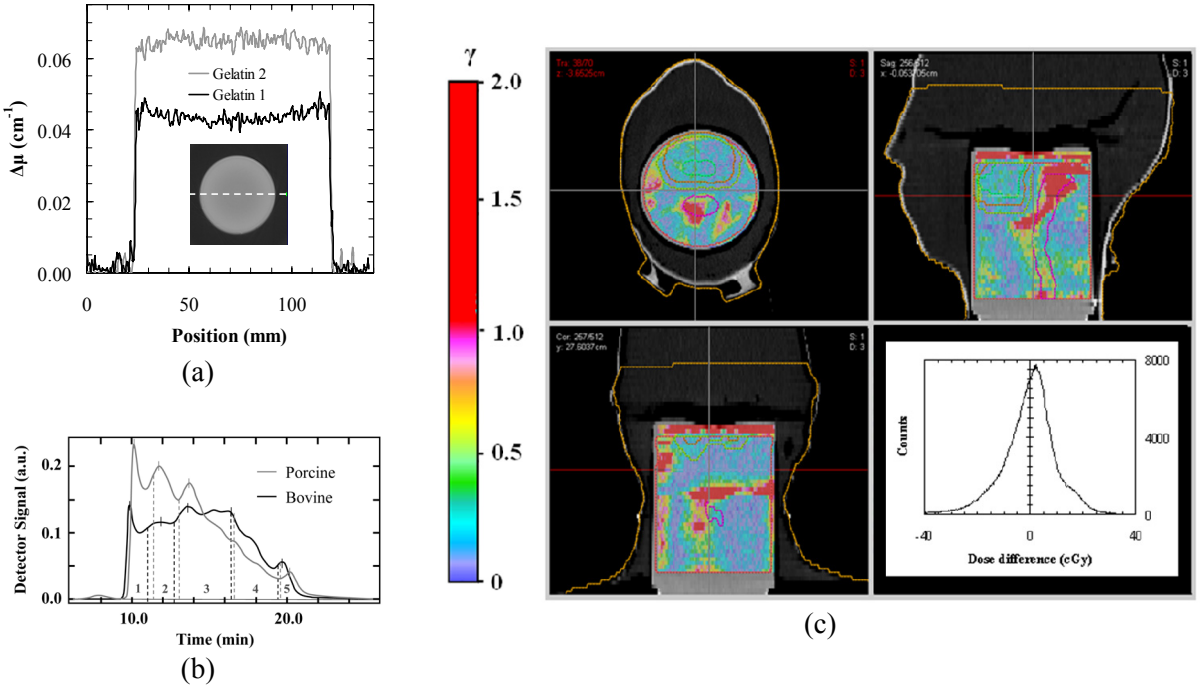

Figure 3: (a) Profiles across the reconstructed optical CT images of the 5 wt% gelatin-in water-filled 1 L PETE jars, prepared using standard 300 bloom porcine skin gelatin (Gelatin 1, black line) and 300 bloom bovine bone gelatin (gelatin 2, grey line), and imaged on the Vista scanner. (b) Size exclusion chromatograms of the two gelatin materials. (c) A 3%, 3mm Low's gamma function analysis of a 200 cGy, 6 MV IMRT treatment fraction delivered to a bovine gelatine-based FXG-gel dosimeter in-phantom. (c, bottom right inset) A dose difference histogram of the delivery, comparing treatment plan and gel-measured dose.

standards to infer the molecular weight from the hydrodynamic volume, which is related to effective particle size. Regions 1-5 in figure 3b correspond to the molecular weight ranges of >250 kilodaltons (kDa), 250-150 kDa, 150-50 kDa, 50-20 kDa, and 20-4 kDa respectively.

An IMRT study was then completed using a wax-filled reproduction of the head-and-neck from a Kyoto SBU-4 Rando anthropomorphic phantom (Capintec, Ramsey, NJ, USA) prepared at the Cancer Centre of Southeastern Ontario with a custom cavity designed to fit the standard 1 L PETE jar gel dosimeter. Two 1 L PETE containers were filled from a single batch of bovine gelatin-based FXG gel. One container was irradiated with a well characterized 12 MeV electron beam using the Varian Clinac 21iX linear accelerator and used for dose-to-attenuation calibration. The other container was inserted into the wax-filled Rando reproduction as the IMRT measurement dosimeter. A 6 field, 6MV, 200 cGy IMRT treatment fraction was then planned and delivered (using the same accelerator) to the phantom. The IMRT evaluation is not described in detail here, but is outlined more fully in a companion paper found in these proceedings. Figure 3c presents the results of a 3D Low's gamma function [4] voxel-by-voxel comparison of gel-measured dose against the reference treatment plan dose for the IMRT delivery, employing 3% dose difference and 3 mm distance-to-agreement criteria. Slightly more than 95% of the voxels within the central 8 cm diameter and 10 cm high preferred evaluation volume of the FXG dosimeter [1] satisfy the 3%, 3 mm criteria between the plan dose and gel-measured IMRT dose. The inset plot in the lower corner of figure 3c shows the dose difference histogram comparing treatment plan dose and gel-measured dose for this delivery.

3. Discussion & Conclusions

Referring to figure 1a, most of the raw dose-to-attenuation calibration data are seen to visually overlap in the plot. The fact that the dose-to-attenuation calibration data presented in the inset of figure 1a agree within error gives good indication that a measurement dosimeter can be well-calibrated by a

second FXG gel-filled 1 L PETE jar dosimeter prepared from the same gel batch. In addition to indicating good reproducibility, the overlapping calibration data for the different beam energies shown in figure 1a also suggest that the FXG gel dosimeter is approximately energy independent into the kilo-voltage energy range. As a standard practice then, a dose-to-attenuation linear fit obtained from a well-characterized photon or electron beam delivered to a FXG gel dosimeter can be used to calibrate a second dosimeter prepared from the same gel batch and irradiated with different beam energy.

The results presented in figure 2a suggest that close attention to the time between dosimeter irradiation and scanning is important, as the attenuation is still changing throughout the dosimeter at a rate of ~0.5% every 10 minutes past the 30 minute mark, consistent with Kelly *et al* (1998). In order to reduce the uncertainties introduced by diffusion, it is desirable to minimize the time between irradiation and imaging of the dosimeter. However, the rate of dose development before the 30 minute mark is higher [3], which increases intra-scan variation in attenuation. A good balance between these two parameters is found by choosing a standard wait time between dosimeter irradiation and scanner readout of 30 minutes, measured to within ± 30 seconds. The importance of the fast optical cone beam scan time of 4-5 min is highlighted through these results.

Looking at figure 2b, the depth dose data indicate significant temperature dependence of the optical attenuation. This thermo-chromic behavior is believed to be primarily sourced in d-orbital spin state crossover of the ferric ion in the ferric ion-xylenol orange dye complex with increase in temperature [5]. The increase in attenuation with temperature (from the day 1 scan data) was observed to be approximately 4% per degree Celsius, suggesting that the dosimeter and scan bath temperatures should be matched and controlled to within the practical measurement limit of $\pm$ 0.1^{o}C.

Substitution of the standard use 300 Bloom porcine skin gelatin with a high optical clarity 300 Bloom bovine bone gelatin in the FXG gel dosimeter formulation has the effect of reducing one of the main sources of stray light perturbation in the optical measurement system. The stray light-derived cupping artefact normally observed when using porcine gelatin (figure 3a) is reduced after bovine bone gelatin substitution (and other measurements not presented in this work are consistent with this conclusion). This is likely due to the difference in the effective particle size distributions of the two gelatin materials (figure 3b), which affects the optical attenuation (dose) readout. The overall result is then to reduce the stray light-induced shift (figure 3c inset plot) in the dosimetry normally observed with the use of the standard porcine gelatine [1,2], and to improve the FXG gel measurement of dose (figure 3c) to the target level of 95% voxel agreement using 3%, 3mm Low's gamma function criteria.

Acknowledgements
Research funding for this work has been provided by the Canadian Institutes of Health Research (CIHR) and the Cancer Centre of Southeastern Ontario.

References
[1] Olding T, Holmes O and Schreiner L J 2010 Cone beam optical computed tomography for gel dosimetry I: scanner characterization *Phy. Med. Biol.* **55** 2819-40
[2] Babic S, Battista J and Jordan K 2008 Three-dimensional dose verification for intensity-modulated radiation therapy in the radiological physics centre head-and-neck phantom using optical computed tomography scans of ferrous xylenol-orange gel dosimeters *Int. J. Radiat. Oncol. Biol. Phys.* **70** 1281-91
[3] Kelly B G, Jordan K J and Battista J 1998 Optical CT reconstruction of 3D dose distributions using the ferrous- benzoic-xylenol (FBX) gel dosimeter *Med. Phys.* **25** 1741-50
[4] Low D A and Dempsey J F 2003 Evaluation of the gamma dose distribution comparison method *Med. Phys.* **30** 2455-64
[5] Wulfsberg G 2000 *Inorganic Chemistry* (Sausalito: University Science Books) p 368